

Brownian dynamics simulations for interacting colloids in the presence of a shear flow

Weige Xue and Gary S. Grest

Corporate Research Science Laboratory, Exxon Research and Engineering Company, Annandale, New Jersey 08801

(Received 27 March 1989)

We have carried out Brownian dynamics simulations to measure the self-diffusion of charged colloids in the presence of an oscillating shear flow. We observe that in the two directions perpendicular to the shear velocity direction, the diffusion constant increases monotonically with the shear rate γ . We also find a slight layering along the shear direction. Our results are compared to the forced Rayleigh scattering experiments of Qiu *et al.* [Phys. Rev. Lett. **61**, 2554 (1988)].

Recently, there have been a number of interesting experimental investigations of the properties of colloidal suspensions¹ in the presence of an oscillatory or steady shear flow.²⁻⁵ Because the particle spacings for these charge-stabilized suspensions are on the scale of 10^3 to 10^4 Å, the energy density and elastic constants are 10^9 to 10^{12} times smaller than conventional atomic systems. This means that at shear rates γ which are readily achievable in the laboratory, it is possible to perform experiments where the applied stresses are comparable to the energy density. As a result, many new phenomena, including shear-induced melting,² laser-induced freezing,³ and shear-induced order⁴ have been observed. While a number of theoretical⁶ and computational studies^{7,8} of the effect of high shear rate for atomic fluids have been reported, it is not clear whether these studies can be applied to suspensions. In particular, they do not take into account the liquid in which the particles are suspended, either in terms of its contribution to the suspension viscosity or in terms of the hydrodynamic interaction which may be important at high shear rates. Furthermore, Evans and Morriss⁹ have recently shown that the shear-induced order of atoms into "strings" aligned parallel to the flow velocity observed in several nonequilibrium molecular-dynamics (NEMD) simulations⁷ arises from the use of a thermostat which assumes a stable linear velocity profile. The use of a thermostat which does not bias the streaming velocity profile causes the string phase to vanish.

In this paper, we present the first Brownian dynamics simulations¹⁰ of charge-stabilized polystyrene sphere (polyballs) suspensions in the presence of an oscillating shear flow. Because the polyballs are large (> 300 Å) compared to the surrounding fluid molecules, we treat the fluid as a viscous medium in which the motions of the polyballs are overdamped and since the volume fraction is low, we ignore hydrodynamic interactions. In this paper, we study the self-diffusion of polyballs in the liquid state driven far from equilibrium by an oscillating shear flow and compare our results to recent forced Rayleigh scattering experiments of Qiu *et al.*⁵ We find, in agreement with their work, that aside from the usual enhancement of the diffusion due to Taylor dispersion¹¹ in the shear velocity direction, there is an additional contribution to the diffusion coefficients D_i in all three directions which increases as the shear rate γ increases. We find that for small γ , the self-diffusion coefficients in the two directions

the flow direction increase monotonically approximately as $\gamma^{1/2}$ and seem to saturate at large γ to a value near that for noninteracting particles $D_0 = k_B T / 6\pi\eta R$, where T is the temperature, k_B is Boltzmann's constant, R is the radius of the polyball, and η is the viscosity of the fluid.

The system we considered consists of N identical spheres of radius R , dispersed in a fluid of dielectric constant ϵ at temperature T . Alexander *et al.*¹² have shown that in the dilute limit, the interaction between polyballs can be treated by a repulsive Yukawa potential in which the polyballs interact with a renormalized charge Z^* which differs from their bare charge Z ,

$$U(r) = Z^{*2} e^2 e^{2\kappa R} (1 + \kappa R)^{-2} e^{-\kappa r} / \epsilon, \quad (1)$$

where ϵ is the background dielectric constant and κ is the inverse screening length. κ can be increased by adding counterions to the fluid. The simulations are carried out using the Brownian dynamics method of Ermak¹³ which is based on the Smoluckowski equation. In the nonshear situation and the absence of hydrodynamic effects this method has been well understood and used in many areas.¹⁰ The particle trajectories at time $t + \Delta t$ are determined by

$$\mathbf{r}_i(t + \Delta t) = \mathbf{r}_i(t) + (D_0/kT)\mathbf{F}_i(t)\Delta t + \mathbf{W}_i, \quad (2)$$

where $\mathbf{F}_i(t)$ is the force on particle i from the remaining particles and each component of the random force \mathbf{W}_{ia} is chosen independently from a Gaussian distribution with zero mean and variance $\langle \mathbf{W}_{ia}(t)^2 \rangle = 2D_0\Delta t$ and D_0 is the free diffusion constant. We choose the time step Δt to be $0.005\tau_0$, where τ_0 is the time for a noninteracting polyball to diffuse a distance $a = (N/V)^{-1/3}$, the mean interparticle spacing. This time step was sufficiently small to insure that the system remained stable, even when the shear flow was added. We also used periodic boundary conditions in all three directions, and set the interaction to zero for all particle pairs separated by a distance greater than $3/\kappa$.

For definiteness, we choose parameters to be comparable with the experiments by Dozier and co-workers,¹⁴ who measured the diffusion coefficient D/D_0 at room temperature of a colloidal suspension without shear. In his study, $R = 0.038$ μm and volume fraction $\phi = 5$ vol%. By varying the amount of HCl, $\lambda = \kappa a$ was varied from 2 to 12. We made a number of runs for different values of κ and Z^* , and found that $Z^* = 200$ gave good agreement between

our results for the long-time diffusion constant

$$D \equiv \lim_{t \rightarrow \infty} \frac{1}{t} \sum_{i=1}^N \langle [r_i(t) - r_i(0)]^2 \rangle / 6tN$$

and that of Dozier and co-workers. Here the average is taken over at least 20 starting configurations 1000 steps apart. We then subjected a system of $N = 500$ particles with $\lambda = 3$ to a shear flow by shearing the box while keeping the volume constant. Similar to the experiments, we applied an oscillating shear to the system with frequency ω and amplitude A . This was done by adding an additional shear contribution¹⁵ to the right-hand side of Eq. (2), $\mathbf{r}_{si} = \hat{\mathbf{e}}_x A z_i \Delta t \sin(2\pi\omega t)$. Here A is the maximum displacement along the shear velocity direction (x) by which two particles can be separated due to shear flow if the distance between them is one unit along the z direction, as shown in the inset to Fig. 1. Since we kept the bottom of the box fixed, AL_z is the maximum displacement of the top of the box. As before, we used periodic boundary conditions in all three directions except now if a particle exited from the top, it was introduced at the bottom with a shift $AL_z \sin(2\pi\omega t)$, where L_z is the box size. The displacement of a particle due to the shear flow is $(Az \sin(2\pi\omega t), 0, 0)$ at time t . The average shear rate can then be defined as

$$\bar{\gamma} = \langle dx/dt \rangle / z = 2\pi A \omega \langle \cos(2\pi\omega t) \rangle = 4A\omega,$$

where the average is over $\frac{1}{4}$ of a cycle. In our simulation, the amplitude A ranged from 1 to 8 and the largest ω was $2/\tau_0$. In contrast to the earlier MD simulations,^{7,8} no thermostat was needed in our Brownian simulations, because of the strong damping of the particles.

The relevant dimensionless number which characterizes the importance of convection and diffusion is the Péclet number $P_c = a^2 \gamma / D$. In most of our runs, we are in the

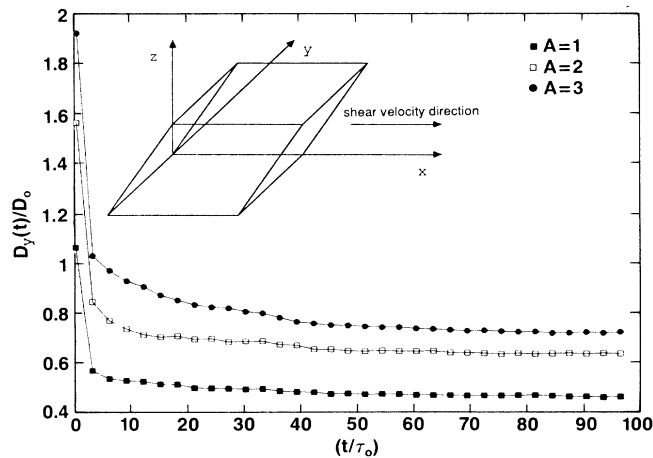


FIG. 1. Diffusion coefficient as a function of time at different shear amplitude for fixed frequency $\omega = 2/\tau_0$. $D_y(t)$ is calculated from the results for long time ($> 50000\Delta t$) and averaged over many initial configurations. The inset shows the coordinate system in which the shear flow velocity is along the x axis and the shear direction is along z . The shear rate is linear along z direction and does not change in y direction.

limit where the motion of the particles is largely convective rather than diffusive and $P_c < 16$. For our largest γ , in the time it takes a polyball to diffuse a distance a above or below the constant velocity plane, it has been convected a distance of $16a$. In most cases near-neighbor particles transverse many times the near-neighbor separation a in a cycle.

In our shear simulations, we first tested that the mean-squared displacement is linear in time and that a well-defined diffusion coefficient D exists. Because of the shear, D is anisotropic and we measured three diffusion coefficients, D_x , D_y , and D_z , which are the long-time limit of $D_i(t)$, where for example, $D_y(t) \equiv \sum_{i=1}^N \langle [y_i(t) - y_i(0)]^2 \rangle / 2Nt$, and similarly for $D_z(t)$. For $D_x(t)$, we have to subtract out the contribution due to the convection term. A simple way this can be done is to calculate

$$D_x(t) = \sum_{i=1}^{N'} [x_i(t) - x_i(0)]^2,$$

where the prime means that only times t such that $\sin(2\pi\omega t) = 0$ are included. To obtain accurate results for these diffusion coefficients, we made very long runs of order $(5-10) \times 10^4 \Delta t$ and averaged over many initial configurations after discarding the first $(2-4) \times 10^4 \Delta t$ for equilibration. Sample results for the time-dependent diffusion coefficient are shown in Fig. 1. From plots of this type, we determined that the long-time diffusion constants $D_i \equiv \lim_{t \rightarrow \infty} D_i(t)$ presented in Fig. 2 are accurate to within 10%.

As the amplitude A increases, we find that the diffusion constants increase monotonically. For the nonsheared case, the diffusion constant is isotropic and equal to about $\frac{1}{3}$ of the noninteracting value. In a shear flow, the diffusion along the shear velocity direction (x axis) is difficult to determine accurately, but from the data we have, we can say that there is a well-defined diffusion constant (D_x) under shear flow, and that it increases monotonically with the shear rate. Here we concentrate only on the diffusion coefficients in the two perpendicular directions, y and z . We can see from Fig. 2, that both D_y and D_z increase monotonically, and D_y is always larger than D_z . At small shear rates, both D 's increase faster than linearly, approximately as $\gamma^{1/2}$. The solid lines in Fig. 2 are best fits to a $\gamma^{1/2}$ dependence, which describe the data fairly well for D_y . We have calculated the diffusion constants for the same shear rate at several combinations of A and ω and find that as long as $A > 1$, D_y and D_z depend only on γ , not on ω and A separately. One possible explanation of the difference between D_y and D_z is that as γ increases, there is a slight layering of the structure and the particles find it is easier to diffuse within the layer than across the layers. The diffusion in the z direction would then be suppressed because openings in a layer move faster than particles can get into them.

The overall increase of the diffusion coefficients seems to be partially due to a reduction of the effective interaction under shear. That is, as the neighbors of a particle are moving rapidly by it, the effective interaction is reduced. We measured the isotropic pair correlation function $g(r)$ and found an overall reduction in the height of the first peak as γ increased, though the position of the

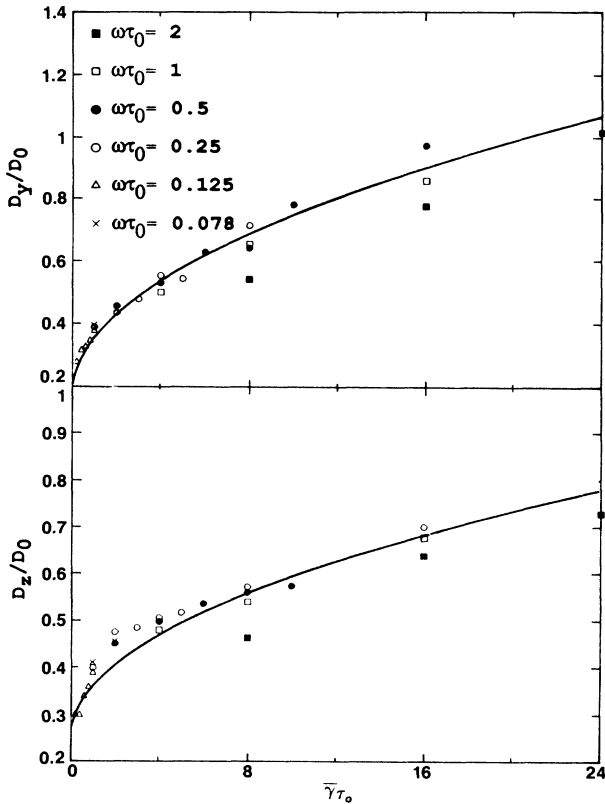


FIG. 2. Diffusion coefficients as a function of the shear rate. The shear rate is composed of the amplitude A and frequency ω , $\bar{\gamma}=4A\omega$. At each shear rate, we have used several different combinations of the amplitude and frequency. Upper figure is the diffusion coefficient D_y and the lower one is D_z . D_y saturate at $\bar{\gamma}\tau_0 \sim 24$, and D_z saturates at higher rate $\bar{\gamma}\tau_0 \sim 40$. D_y is always larger than D_z . The solid lines are a best fit to a $\gamma^{1/2}$ dependence.

peak remained unchanged. The results of our simulations are very similar to the experimental results of Qiu *et al.*⁵ except that they found that D_y increases linearly with the shear rate even for small values of γ . The difference in the shear rate dependence of D_y between our results and Qiu's is probably due to the difference of the wave-front profile in the two cases. In the forced Rayleigh scattering experiments the wave front is nonuniform and the effective shear rate is an average of many shear rates, while in our case the profile is uniform.

We also calculated the structure factor $S(\mathbf{k})$. Since the system is anisotropic under shear flow, we calculated the anisotropic structure factors $S(\mathbf{k})$. $S(k_y)$ is calculated by choosing the k vector to be parallel to the y direction. From Fig. 3, we can see that $S(k_y)$ is practically unchanged under shear flow and shows no evidence of string ordering. We also checked this directly by examining the trajectories of many of the particles in the system as well as examining projections of the particle positions on the y - z plane, and did not observe any evidence for string ordering under shear flow. This should probably not be surprising because our systems are rather dilute and far from the melting temperature.

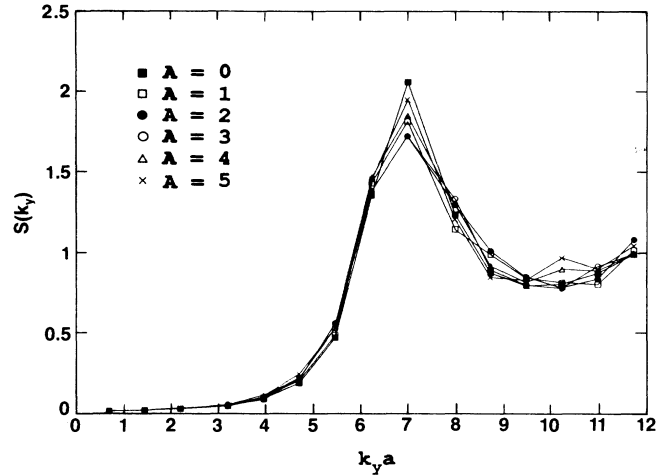


FIG. 3. The anisotropic structure factor in the y direction $S(k_y)$ vs $k_y a$ for various shear rates for $\omega=0.5/\tau_0$. Here a is average near-neighbor distance. We can see the difference between the five curves is within the noise indicating that $S(k_y)$ is unchanged under shear flow.

We determined the structure factor along the z direction $S(k_z)$, and found that, consistent with our results for D_y and D_z , there is some layering under shear flow. The first peak of $S(k_z)$ increases with the shear rate monotonically, as seen in Fig. 4. For zero shear, our uncorrelated liquid phase has a peak height of about 1.5. We find that the peak height increases with the shear rate (inset in Fig. 4) and the width of the peak also increases. This result indicates that while there is some layering along the shear gradient direction (z), the distance between the layers is quite broadly distributed. By examining the trajectories

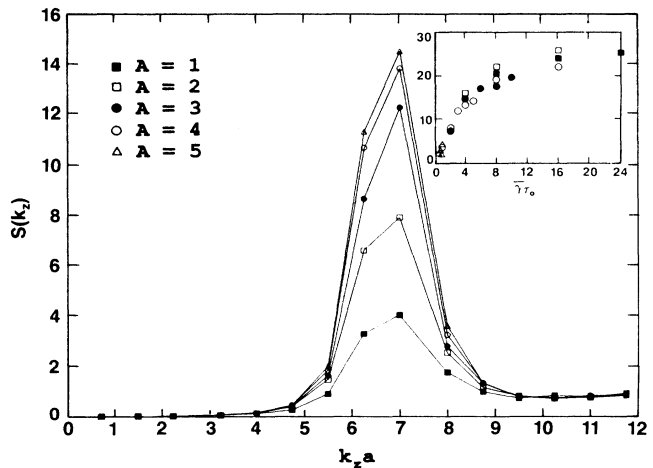


FIG. 4. Structure factor $S(k_z)$ vs $k_z a$ for various shear amplitudes with $\omega=0.5/\tau_0$. The inset shows the height of the first peak as a function of shear rate, which increases monotonically and then saturates for large $\bar{\gamma}$. The width of the peak also increases as the shear rate increases. Note that while the peak position is unchanged, the peaks become more unsymmetric as the shear flow increases.

of the particle motion, we have some evidence that the particles move more easily in the x - y plane than along z direction across the plane. This phenomena is consistent with the diffusion-coefficient calculations.

From our Brownian dynamics simulation of the charged colloidal suspensions under the shear flow, we can conclude that the anisotropic diffusion coefficients D_y and D_z increase monotonically as γ increases with the rate of increase decreasing for large shear γ . For $\bar{\gamma}\tau_0 > 24$, we found that D_y/D_0 may actually become greater than 1, while D_z/D_0 only reaches 1 for $\bar{\gamma}\tau_0 \approx 40$. The fact that D_y/D_0 exceed 1 may be possible since the rapid motion of particles past one another could lead to an effective increase in the "random" noise they experience such that the diffusion increases to values even greater than the noninteracting diffusion value. The largest shear rate we can achieve at the present time is $\bar{\gamma}\tau_0 \sim 40$. For larger amplitude and high frequencies, we have difficulty keeping the simulation stable. Experimentally,⁵ it appears

that D_y may be saturating near its noninteracting value D_0 , though D_y/D_0 exceeding 1 is not ruled out. Further experiments and simulations in this high shear rate regime are needed to clarify whether the diffusion constant can actually become larger than its noninteracting value. While the parameters (particle size, charge, concentration, etc) in the experiments⁵ and in our simulations were in fact quite different, the range of shear rate (in dimensionless units) and the behavior of D_y in this range are quite similar. It is interesting to speculate that when expressed in dimensionless units, D_y/D_0 vs γ may be universal, independent of the detailed parameters. This observation is presently under further investigation. Finally, by calculating the anisotropic structure factor $S(\mathbf{k})$, we find that we do not observe any string ordering under the shear, but only a slight layering along z direction.

We would like to thank Paul Chaikin, David Pine, Mark Robbins, and Xia Qiu for helpful discussions.

-
- ¹P. Pieranski, *Contemp. Phys.* **24**, 25 (1983); W. Van Megen and I. Snook, *Adv. Colloid Interface Sci.* **21**, 119 (1984); P. M. Chaikin, J. M. DiMeglio, W. D. Dozier, H. M. Lindsay, and D. A. Weitz, in *Physics of Complex and Supermolecular Fluids*, edited by S. A. Safran and N. A. Clark (Wiley, New York, 1987), p. 65.
- ²B. J. Ackerson and N. A. Clark, *Phys. Rev. Lett.* **46**, 123 (1981); R. L. Hoffman, *J. Colloid. Interface Sci.* **46**, 491 (1974).
- ³A. Chowdhury, B. J. Ackerson, and N. A. Clark, *Phys. Rev. Lett.* **55**, 833 (1985).
- ⁴B. J. Ackerson and P. P. Pusey, *Phys. Rev. Lett.* **61**, 1033 (1988).
- ⁵X. Qiu, H. D. Ou-Yang, D. J. Pine, and P. Chaikin, *Phys. Rev. Lett.* **61**, 2554 (1988).
- ⁶T. R. Kirkpatrick and J. C. Nieuwoudt, *Phys. Rev. Lett.* **56**, 885 (1986).
- ⁷J. J. Erpenbeck, *Phys. Rev. Lett.* **52**, 1333 (1984); L. V. Woodcock, *ibid.* **54**, 1513 (1985); D. M. Heyes, G. P. Morriss, and D. J. Evans, *J. Chem. Phys.* **83**, 4760 (1985); S. Hess, *Int. J. Thermophys.* **6**, 657 (1985).
- ⁸J. Rainwater, H. J. M. Haley, N. A. Clark, and B. J. Ackerson, *J. Chem. Phys.* **79**, 4448 (1983).
- ⁹D. J. Evans and G. P. Morriss, *Phys. Rev. Lett.* **56**, 2172 (1986).
- ¹⁰K. Gaylor, I. Snook, and W. van Megen, *J. Chem. Phys.* **75**, 1682 (1981); K. J. Gaylor, I. K. Snook, W. van Megen, and R. O. Watts, *J. Phys. A* **13**, 2513 (1980); G. Nagele, M. Medina-Noyola, and R. Klein, *Physica* **149A**, 123 (1988).
- ¹¹G. I. Taylor, *Proc. R. Soc. London, Ser. A* **219**, 186 (1954); **223**, 446 (1954).
- ¹²S. Alexander *et al.*, *J. Chem. Phys.* **80**, 5776 (1984).
- ¹³D. L. Ermak, *J. Chem. Phys.* **62**, 4189 (1975); **62**, 4197 (1975).
- ¹⁴W. D. Dozier, Ph.D. thesis, University of California, Los Angeles, 1986 (unpublished); W. D. Dozier, H. M. Lindsay, and P. M. Chaikin, *J. Phys. (Paris) Colloq.* **46**, C3-165 (1985).
- ¹⁵This generalization of Eq. (2) to the case of nonzero shear, seems to us to be physically reasonable, but we have not attempted a direct justification of the equation.